AN EXPERIMENTAL SIMULATION OF LIQUID FUEL INJECTION INTO A HEATED SUBSONIC GAS CROSSFLOW

by

Patrick William Hewitt

Thesis submitted to the Faculty of the

Virginia Polytechnic Institute and State University

in partial fulfillment of the requirements for the degree of

MASTER OF SCIENCE

in

Aerospace and Ocean Engineering

APPROVED:

J. A. Schetz, Chairman

A. K. Jakubowski

W. F. O'Brien

September, 1982

Blacksburg, Virginia

Acknowledgement

This work was supported by the Air Force Office of Scientific Research with Dr. B. T. Wolfson as Technical Monitor.

TABLE OF CONTENTS

	Page
ACKNOWLEDGEMENT	ii
TABLE OF CONTENTS	iii
LIST OF FIGURES	v
LIST OF TABLES	vi
NOMENCLATURE	viii
I. INTRODUCTION	1
II. EXPERIMENTAL METHOD	7
A. Test Matrix and Parameters	7
B. Spark Shadowgraphs	8
C. Streak Photographs	8
D. Droplet Size Distribution	8
III. EXPERIMENTAL APPARATUS	10
A. Test Facility	10
B. Injection System	10
C. Photographic Equipment	11
IV. DIFFRACTIVELY SCATTERED LIGHT METHOD APPARATUS	13
V. RESULTS AND DISCUSSION	17
A. Jet Plume Structure	17
B. Penetration	18
C. Droplet Size Distribution	19
VI. CONCLUSIONS	23
REFERENCES	24

TABLE OF CONTENTS (CONT'D)

	Page
TABLES	26
FIGURES	31
VITA	50

LIST OF FIGURES

Figure		Page
1	Freon-12 Delivery System	31
2	Injector Assembly	32
3	Spark Shadowgraph Apparatus	33
4	Streak Photograph Apparatus	34
5	Theoretical Illumination Profile	35
6	Optical System for DSLM	36
7	Optical Arrangement for DSLM	37
8	Block Diagram of Data Processing	38
9	Versi-Tech Plot of Recorded Data	39
10	Spark Shadowgraphs Water - $\bar{q}$ = 1 and 4	40
11	Spark Shadowgraphs Freon-12 - $\bar{q}$ = 4	41
12	Spark Shadowgraphs Freon-12 - $\bar{q}$ = 1	43
13	Sample Streak Photograph	45
14	Penetration Plot	46
15	Droplet Distribution in Plume Water - $\bar{q}$ = 1 and 4	47
16	Droplet Profile at $\bar{x}$ = 100 Freon-12, $\bar{q}$ = 4	48
17	Droplet Profile at $\bar{x}$ = 100 Freon-12, $\bar{q}$ = 1	49

LIST OF TABLES

Table		Page
I	Variation of Injection Parameters	25
II	Test Matrix	26
III	Droplet Distribution in Plume Water-$\bar{q}$ = 1 and 4	27
IV	Droplet Profile at $\bar{x}$ = 100 Freon-12, $\bar{q}$ = 4	28
V	Droplet Profile at $\bar{x}$ = 100 Freon-12, $\bar{q}$ = 1	29

NOMENCLATURE

$\bar{q}$	jet/freestream momentum flux ratio $(\rho_j V_j^2/\rho_\infty V_\infty^2)$
ρ	density
V	velocity
x	downstream coordinate from injector
$\bar{X}$	$\frac{x}{d_j}$
y	vertical coordinate
$\bar{y}$	y/d_j
d_j	jet diameter
D	mean droplet diameter
θ	scattering angle
$I(\theta)$	normalized intensity function
f	focal length of lens
d	traverse distance
$\bar{\theta}$	reduced scattering angle
λ	wavelength of laser light
h	penetration of plume
M	Mach number
σ	Cavitation Number
T*	normalized Temperature Difference
T	temperature
p_v	vapor pressure
p	pressure

Subscripts

j	refers to jet conditions
∞	refers to freestream conditions
o	refers to freestream stagnation conditions
$( )_{pro}$	prototype conditions
$( )_{sim}$	simulated conditions

I. INTRODUCTION

Fuel jet injection plays a major role in the design of air-breathing engines such as ramjets or scramjets. Extensive studies must be conducted into the mechanisms of combustion and the effects of various injection parameters. This information is also valuable in the areas of thrust vector control, afterburners, liquid surface injection for cooling purposes and external burning in the wake of projectiles. In the case of ramjet or scramjet engines, the fuel is usually injected from a wall or strut across an airflow. This paper will address a problem associated with liquid injection perpendicular to a subsonic airstream, a case which arises in the design considerations of ramjet engines.

Much work has been done on the mechanisms of jet decomposition, penetration of the liquid into the freestream and atomization of the injectant. (Refs. 1-8). Comprehensive reports by Schetz and Padhye (Ref. No. 9) and Forde (Ref. No. 7) cover the effects of injection parameters and provide data correlations. Reichenbach (Ref. No. 10) has studied the effects of injectant physical properties on jet structure, and Nejad and Schetz (Ref. No. 11) have extended their studies to include droplet sizes in the plume. Additionally Adelberg (Ref. No. 12) has contributed an analytical prediction of droplet sizes for given injection conditions. All of this work has been performed in a cold flow situation, where ambient temperature injectant is injected into ambient air and evaporation along the plume is not considered.

In order to take one step closer to the simulation of actual fuel injection in a hot-flow situation, where ambient temperature fuel is injected into a heated airstream, this work will introduce the effects of evaporation and heating of the injectant along the plume by the airflow. The effect on droplet sizes, penetration, and jet structure will be investigated. This represents a significant advance in injection research even without consideration of droplet burning, since some combustor processes require fuel sprays to be completely vaporized and mixed with air before reaction occurs in the combustion chamber. Therefore, fundamental data are required on droplet vaporization in heated gas streams (Ref. No. 13). Detailed experimentation under the actual conditions to be encountered in a ramjet combustor is difficult and very expensive. To permit careful, laboratory-environment studies covering a wide range of the important variables and parameters, a rational simulation procedure that allowed use of an unheated air stream would be valuable.

The simulation problem that we wish to address can be stated as follows. If all the mechanical aspects of the prototype and model injection problems are matched except heating, how can the effects of heating and thus vaporization along the plume be simulated with an ambient temperature air flow? Thus, we will require at least close matches of: injector size and shape, injectant flow rate (expressed as $\bar{q} \equiv \rho_j V_j^2/\rho_\infty V_\infty^2$), crossflow Mach number and injectant density, viscosity and surface tension. This would be enough to insure equivalence if heating were not important. In the prototype case, ambient temperature fuel (e.g. Kerosene) is injected across a hot air stream. At the in-

jection temperature, the vapor pressure is low, and there is little evaporization. As the liquid is heated along the trajectory of the jet, the vapor pressure rises rapidly, and there is substantial evaporization. There is, therefore, some time history of temperature (and vapor pressure) along the plume, and that is the process that we wish to simulate.

To put this all on a rational basis, we must introduce non-dimensional expressions involving the vapor pressure and the driving force for heating - the difference between the injection temperature and the air stagnation temperature. The relevant reference point for the local vapor pressure is the static pressure, and this difference can be normalized with the dynamic pressure, so we choose the parameter

$$\sigma(T) \equiv \frac{p_v(T)-p_\infty}{\frac{1}{2}\rho_\infty V_\infty^2}$$

This can be recognized as what is often termed a Cavitation Number in a different context. For a suitable dimensionless temperature difference, we choose simply

$$T^* \equiv \frac{T_{o,\infty}-T_j}{T_{o,\infty}}$$

By physical reasoning then, we have developed a simulation procedure that requires matching all the mechanical parameters mentioned earlier and now T^* and $\sigma(T_j)$ and $\sigma(T_{o,\infty})$. This latter point is the condition that the liquid jet tends toward as it is heated along the trajectory.

For this investigation, an example case was chosen to demonstrate how these parameters can be used to create a simulation of a real case of fuel injection. Consider a ramjet engine traveling at a freestream Mach number of 2.1 at 60,000 ft. Assuming diffusion to a Mach number of 0.44 in the combustor yields a stagnation temperature of 405°K in the combustor entrance plane and a stagnation pressure of 0.884 atm. Now consider Kerosene fuel injected at 25°C. At this point p_v = 0.033 atm so,

$$(\sigma_j)_{pro} = -5.7$$

$$(T_j^*)_{pro} = 0.26$$

After injection, but before combustion begins, the fuel will be heated and begin the vaporization process. The maximum value the fuel would be heated to would be the freestream stagnation value of 405°K. At this temperature, the vapor pressure of Kerosene is 2.993 atm, and

$$(\sigma_\infty)_{pro} = 17.6$$

$$(T_\infty^*)_{pro} = 0$$

This establishes the endpoints in the heating process for the hot-flow case and the basis for the flow problem to be modelled. The task now becomes transforming the process into one which can be implemented in a cold-flow wind tunnel facility.

The wind tunnel freestream Mach number was taken as the same as that in the combustor for the real case, M = 0.44. In establishing

a value for stagnation pressure, a compromise must be reached between operable values for the wind tunnel available and the satisfaction of matching requirements. A value of 2.517 atm adequately satisfied these needs, generating the pressure ratios which enter in a later discussion. This value fixes the freestream static and dynamic pressures at 2.204 and 0.313 atm respectively. The stagnation temperature of the facility was that of ambient air or 25°C. With these figures to work with, a fluid must be found such that the values of σ and T* are matched with the real case at injection and at tunnel stagnation conditions.

The first fact that presents itself is that at injection the value of $(T^*)_{sim}$ must be 0.26. Since the wind tunnel stagnation temperature is known, this fixed the injection temperature at -50°C. Therefore, a model fluid had to be found with a vapor pressure of 0.422 atm at -50°C in order to match the conditions at injection $(\sigma_j)_{sim} = (\sigma_j)_{pro} = -5.7$. Freon-12 is found to have a vapor pressure of 0.388 atm at -50°C. Additionally the model fluid must have a vapor pressure of 7.483 atm at 25°C in order to match end point conditions $(\sigma_\infty)_{sim} = (\sigma_\infty)_{pro} = 17.6$. Freon-12 is found to have a vapor pressure of 6.802 atm. at 25°C. This physical property and density are also a reasonable match with Kerosene. Freon-12 would seem to be a good choice, and indeed this was the test fluid selected. The similarity parameters are summarized as follows:

Kerosene Prototype (Hot Flow) Case	Freon-12 Simulated (Cold Flow) Case
$T_j = 25°C$	$T_j = -50°C$
$T_o = 132°C$	$T_o = 25°C$

$\sigma_j = -5.7$

$\sigma_\infty = 17.6$

$T_j^* = .26$

$T_\infty^* = 0$

Viscosity @ T_j = 0.19 centipoise

Specific gravity = 0.8

Surface tension @ T_j = 26 dyne/cm

Heat of vaporization = 77 cal/gm

$\sigma_j = -5.8$

$\sigma_\infty = 15.0$

$T_j^* = .26$

$T_\infty^* = 0$

Viscosity @ T_j = 0.26 centipoise

Specific Gravity = 1.3

Surface tension @ T_j = 19 dyne/cm

Heat of vaporization = 39.5 cal/gram

Now that a simulation, cold flow problem has been posed, the processes of injection can be examined, without the cumbersome and costly equipment necessary for hot-flow testing.

II. EXPERIMENTAL METHOD

A. Test Matrix and Parameters

The most important similarity parameter associated with the fluid mechanics of liquid injection is termed $\bar{q}$, defined as the ratio of jet/freestream momentum flux ratio ($\rho_j V_j^2/\rho_\infty V_\infty^2$). For this investigation, values of $\bar{q}$ = 1 and 4 were chosen for testing. A value of $\bar{q}$ = 4 is known as Regime II injection (Ref. No. 2), and it is a reasonable value for actual liquid fuel injection, and test results may lend themselves to combustor problems. A value of $\bar{q}$ = 1 is classified as Regime I (Ref. No. 2), and results may be directed more in the area of film cooling through surface injection.

In order to completely cover the effects of evaporation, several injection temperatures were studied along with the model value chosen to achieve simulation of the prototype combustor. The Freom-12 was injected at temperatures ranging from 10°C to -50°C. Correspondingly the Cavitation Number varied from 6.3 to -5.8, and the normalized temperature T* varied from 0.06 to 0.26. These values are presented in Table I.

The completed test matrix is shown in Table II. Water was included in the matrix to form a simple baseline case without significant evaporation for comparison. Those results are of value in their own right, since rigorous studies of this type concerning droplet sizes in a subsonic water plume are limited. For each condition, several types of tests were performed.

B. Spark Shadowgraphs

In order to observe the processes of injection and jet decomposition, spark shadowgraphs were taken of the liquid jet in the wind tunnel. A spark shadowgraph is a short duration (10^{-8} sec.) photograph which presents a stop-action look at the flowfield. From these photographs, the actual process of jet break-up can be observed, and in the past these photographs have even been used to determine droplet sizes and distributions in the jet plume.

C. Streak Photographs

The purpose of this procedure was to obtain jet cross-stream penetration measurements at each condition as a function of distance downstream of the injector, $\bar{x}$. Whereas a spark shadowgraph is a stop-action photograph, a streak photograph entails a longer exposure duration (10^{-3} sec.) which effectively integrates the unsteady jet motion over the exposure time. This will render a more representative penetration measurement. The penetration was measured directly from the photographs.

D. Droplet Size Distribution

The third testing survey undertaken was a determination of the mean droplet diameter at various locations in the jet plume. The method chosen to acquire this information was the Diffractively Scattered Light Method (DSLM). Simply stated, this method relates the pattern of scattered light to the mean droplet diameter in a small area of the jet plume. The details of the technique will be discussed

in a later section. The method was used to determine a mean droplet diameter at $\bar{x}$ values of 10, 15, 25, 50, 100 and $\bar{y}$ values chosen according to penetration heights taken from the streak photographs. In this way, the variation of the droplet diameters throughout the plume could be determined.

III. EXPERIMENTAL APPARATUS

A. Test Facility

This study was conducted in the Virginia Tech supersonic wind tunnel. The tunnel is a blow-down type with interchangeable test sections, each with an interior cross-section of 23 cm x 23 cm. For this work a subsonic/transonic section was used. This section has an adjustable, downstream throat facilitating the adjustment of the free-stream Mach number. The Mach number was determined through static pressure taps mounted on the floor of the test section and the stagnation pressure measured upstream in the settling chamber.

High quality fused silica optical flats were used as windows and mounted on movable plates which covered each side of the test section. Such high quality windows were necessary in this investigation so as not to scatter or distort the laser beam used in the DSLM.

B. Injection System

As previously mentioned, water and Freon-12 were chosen as the injectants. Some small differences in jet behavior, penetration, and droplet sizes may occur in the use of hydrocarbon fuels due to a change in surface tension and viscosity (Refs. 11, 14), however, the results have been shown to be similar enough to extend the knowledge to combustion problems.

The water was delivered from a storage tank pressurized with nitrogen, and the mass flow rate was measured with a calibrated Rotameter. Fine adjustments of the flowrate were made with a needle valve.

A slightly more complex arrangement was necessary to deliver the Freon-12 due to the need for careful attention to the injection temperature. The Freon-12 was stored in commercial 30-lb disposable tanks. It then passed through a specially built heat exchanger tank. The heat exchanger consisted of a cast-iron vessel surrounded by Styrofoam insulation containing a bath of ethyl alcohol with an immersed coil of copper tubing through which the Freon-12 was passed. Dry ice was added to the ethyl alcohol until the desired temperature was reached. The temperature of the alcohol was monitored by a thermocouple immersed directly in the bath. The cooled Freon-12 was then passed through a cryogenic Hoffer MF-70 flowmeter to monitor the delivery flowrate. Two Nupro bellows-type cryogenic valves were used to adjust the flowrate. A sketch of the complete delivery system is shown in Fig. No. 1.

The Freon-12 and water were injected into the wind tunnel through a removable injector assembly. The assembly consisted of an insulated central duct leading to a 0.91 mm diameter orifice. A thermocouple was placed directly in the injectant flow in order to monitor the injectant temperature at all times. The injector was fitted flush with the floor of the wind tunnel so as not to create any disturbances in the flowfield., A sketch of the injector assembly is shown in Figure No. 2.

C. Photographic Equipment

To obtain spark shadowgraphs, a Nanopulser flash was used to backlight the plume. The flash duration was approximately 10^{-8} seconds which adequately stopped the action for observation. A 20 cm. focal

length lens was used to focus the image on a Polaroid film carrier. Type 57 Polaroid film was used (ASA 3000) because a high sensitivity was required due to the extremely short exposure time. The arrangement is shown in Fig. No. 3.

A PEK model mercury-arc lamp was used in conjunction with a parabolic mirror to deliver an intense parallel light source for the streak pictures. This light was used to backlight the plume in the test section. The image of the plume was then projected on a Polaroid film carrier fitted with a shutter. Type 55 Polaroid film (ASA 50) was used, since a high sensitivity was not required with the relatively long exposure time (10^{-3} sec.). The complete arrangement is shown in Fig. No. 4.

IV. DIFFRACTIVELY SCATTERED LIGHT METHOD APPARATUS

The method chosen to determine the droplet diameters in the plume was the DSLM. This method relates light scattering to droplet diameters in a spray. The DSLM has many advantages over other possible techniques. Other methods which have been used in the past are

1) injecting molten wax and collecting and measuring the frozen droplets.
2) examining short duration photomicrographs and measuring droplet sizes from the photograph by hand.
3) Holograph methods - either hand interpreted or lately by TV screen and computer.

The DSLM is not subject to many of the difficulties associated with these methods such as the resolution required to view individual drops, and the tedious process of examining and sizing individual drops. It has the advantages of being usable in high air stream and droplet density situations and routine enough to permit many tests to be run, rather than consuming excessive time with data reduction. For a detailed description of the theory behind this method see Refs. (15) - (18).

The information required for this method is light intensity as a function of scattering angle. The intensities are then normalized with the unscattered light intensity in the forward direction ($\theta = 0$), forming a normalized scattering function $I(\theta)$. Once these values are obtained, the mean droplet diameter can be obtained from the theoretical

illumination profile as compiled by Gooderum and Bushnell (Ref. 16) shown in Fig. No. 5.

To utilize this method, an apparatus must be designed which can measure the intensity of light scattered at various angles from a light source passed through the spray. A Spectra-Physics 15 mw. helium neon laser was chosen as the light source because of the high intensity and clean, parallel light. The laser beam was further filtered with a spatial filter which delivered a thin, parallel beam of intense light. The laser beam was passed through the wind tunnel test section, penetrating the jet plume. The windows normally used in the test section were of insufficient quality for this work, and they were replaced with smaller, high quality windows. The two windows and the laser beam had to be perfectly aligned to eliminate interference patterns. Next, a device must be designed to measure the intensity of the light scattered by the plume at various angles to the laser beam. A photo-multiplier assembly was used to measure the light intensity. The assembly consisted of a RCA-C7164R photomultiplier mounted 0.6 cm. behind a plate with 0.15 cm aperture. The unit was enclosed in a tube and mounted on a traverse. The location of the photomultiplier tube along the traverse was recorded with a ten-Turn potentiometer. The scattered light was collected with a 50 cm. focal length lens positioned as shown in Fig. No. 6. Since the plume is located at the focal length of the lens, the scattered light is parallel when it emerges from the lens, and the scattering angle can be related to the traverse position from the relation $\theta = \tan^{-1} (d/f)$. This arrangement worked well for droplet

sizes down to about 15μm, but to measure smaller droplets, it was necessary to scan at greater angles. For this reason, a different optical arrangement was devised as shown in Fig. No. 7. In this scheme, the collecting lens could be placed closer than the focal length, and upon applying basic lens laws, the scattering angle can be found as a function of the traverse distance, d. The light intensity at various angles can then be found by scanning the photomultiplier along the traverse.

Since the voltages obtained upon scanning varied greatly, a logarithmic amplifier was used to process the signal, which facilitated the recording of the illumination profile. By placing the collecting lens a focal length from the photomultiplier assembly, the unscattered parallel light was focused on the aperture, making the extrapolation to $\theta = 0$ much more accurate.

The required information to compute a droplet size is scattering angle and light intensity. Since the information available is the readout from the photomultiplier and the traverse, these figures must be processed to determine a mean droplet diameter. This process is shown schematically in Fig. No. 8. For each scan, the light intensity was plotted as a function of traverse location on a Versi-Tech plotter. A typical plot is shown in Fig. No. 9. From the plot, the values of the log-amp output were recorded for increments on the traverse. The data processing then consisted of several steps:

1) Convert the traverse locations to angles of scattering.

2) Convert the log-amp output voltage to the photo-multiplier

output voltage.

3) Non-dimensionalize each intensity with the intensity at zero-scattering. This forms the intensity profile $I(\theta)$.

4) Compute $\bar{\theta}$ from the mean theoretical illumination profile given $I(\theta)$.

5) Compute the mean diameter from $\bar{\theta}$ and θ.

Roberts and Webb (Ref. 15) have shown that at a value of $I(\theta) = 0.1$ the standard deviation is only 1.74%. Therefore, the diameters reported here will be those corresponding to $I(\theta) = 0.1$.

The accuracy of this experimental procedure was tested in two ways. First, a determination was made of the mean droplet diameter in the spray of a commercial atomizer with the DSLM. This result (26 μm) was compared to that found by the hand-counting micro-photographic technique (24.6 μm). Next, glass beads with a known size ranging from 48-53 μm in diameter were tested. The DSLM indicated a mean diameter of 48 μm, which again exhibits good accuracy.

V. RESULTS AND DISCUSSION

A. Jet Plume Structure

The spark shadowgraphs of water injected at $\bar{q}$ = 1 and 4 are shown in Fig. No. 10. The processes of jet decomposition which have been mentioned previously are evident, such as the formation of short wavelength, high amplitude waves, and the break-up into clumps and then droplets. These processes follow the same general patterns as break-up in a supersonic cross-flow (see Ref. No. 2).

It is the main intent of this work to examine a case where evaporation of the injectant plays an important part in the atomization mechanisms. The first sequence of photographs are spark shadowgraphs of Freon-12 injected at $\bar{q}$ = 4 (Fig. Nos. 11a, b and c). The photographs are arranged in order of increasing injectant temperature. The case in Fig. No. 11a is the simulation of the chosen prototype ramjet case. The first observation to be made is the cloud-like appearance of the plume. This is unlike the water case where the distinct formation of individual droplets is clearly seen. It is possible, however, to view larger droplets in areas where the cloud is less dense. For this reason it would seem that the process of jet decomposition is not an immediate "flashing" of the injectant, but a mechanism similar to that of water. The rapid heating and evaporation of the injectant along the plume accounts for the fog-like appearance of the jet plume.

As the temperature of the injectant is increased, it is seen that the fog is "burned off" at a more rapid rate. This would be likely to

occur since less heating of the injectant is necessary to reach the high evaporation range, and the whole process is hastened. The supposition of similar water-like basic atomization mechanisms will be further substantiated in the droplet survey results.

The second sequence of photographs are spark shadowgraphs of Freon-12 injected at a $\bar{q} = 1$ (Fig. Nos. 12a, b, c and d). In these photographs since the $\bar{q}$ value has decreased from 4 to 1, the Freon-12 is injected at a lower velocity. Fig. No. 12a represents a simulation of the ramjet case at a low $\bar{q}$. The same observations can be made for these areas concerning the mechanisms of jet decomposition. The primary difference for the case of a lower value of $\bar{q}$ is that due to a decreased jet injection velocity, the fluid penetrates less into the freestream and the plume closely follows the wind tunnel floor.

B. Penetration

The purpose of a streak photograph is to determine the physical dimensions of the jet plume. A sample photograph is shown in Fig. No. 13. The most important piece of data obtained from these photographs is the penetration of the jet plume into the freestream. For each case in the test matrix, a streak photograph was taken, and the data was used to determine a judicious placement of droplet diameter sampling. Additionally, the penetration was measured at a location of 20 diameters downstream of the injector for each test case. These results are plotted as non-dimensional penetration (h/d_j) vs. $\bar{q}^{\frac{1}{2}}$ (Fig. No. 4). As can be seen, there is a small reduction in penetration over the range of

conditions from non-evaporating water injection. A slightly higher penetration is noted for the case of Freon-12 at 10°C. This was probably due to intermittent cavitation in the delivery lines causing bursts of fluid to be injected at a greater velocity than intended.

C. Droplet Size Distribution

The next step in the investigation was to obtain a droplet size distribution for the cases studied. The optical arrangement utilized for the DSLM yielded an average droplet diameter in an area the size of the laser beam (.071 cm^2). The results of these measurements are shown in Fig. No. 15 for the case of water at $\bar{q}$ = 1 and 4. The $\bar{x}$ and y/h axes locate the space coordinates along the plume and mean droplet diameters are plotted along the normal axis. Additionally, these values are tabulated in Table III. These results show that for injection at $\bar{q}$ = 4 the larger droplets initially occupy a region close to the upper edge of the plume. As they are carried downstream they become more evenly distributed along the plume centerline and then gradually settle closer to the injection plane. It should also be noted that the droplet diameters are decreasing in the downstream direction as further atomization and evaporation take place.

The results for water injected at $\bar{q}$ = 1 show a slightly different droplet distribution. At all stations considered, the larger droplets remained in the lower portion of the jet plume. Again, as the droplets travel downstream as the mean droplet diameters decrease. It can also be observed that at virtually all stations, the droplets are larger for the

lower injection rate. These results can be generalized as follows:

1) By increasing $\bar{q}$, which is proportional to the jet velocity squared, the degree of atomization is increased, and smaller droplets result.
2) As the downstream distance from the injector increases, the mean droplet diameter decreases
3) The larger droplets eventually migrate to the lower portion of the plume for the case of a higher dynamic pressure ratio, whereas for a lower $\bar{q}$, the larger droplets are always found close to the wall.

The results can be combined with the photographs of the jet plume to convey a complete picture of how the jet plume behaves under these freestream conditions.

As was previously mentioned from the spark shadowgraphs, a cloud of very small droplets surrounds the jet plume when the readily evaporated Freon-12 is injected. This cloud presents severe difficulties for the DSLM. Because the method is based on the scattering of light, the cloud presents problems because of increased absorption of the laser beam and multiple scattering, since the number of droplets is increased greatly. These factors made the DSLM inappropriate in determining any droplet sizes in the early sections of the plume for the test conditions. Droplets can be seen in the spark shadowgraphs, but the majority are obscured by the vapor cloud making droplet measurements from photographs difficult. It was found, however, that measurements with the DSLM could be made farther downstream after some of the cloud had evaporated. The

thinning effect of the vapor cloud was noted by Reichenbach (Ref. No. 10) where it was observed that a plume of highly evaporating injectant became less dense after a location of $x/d_j > 50$. For these reasons measurements were made here at a location of $\bar{x} = 100$.

The results for Freon-12 injected at $\bar{q} = 4$ and $T_j = -10, -30, -50°C$ are shown in Fig. No. 16 and tabulated in Table IV. The results for Freon-12 injected at $\bar{q} = 1$ are shown in Fig. No. 17, and tabulated in Table V. Data for $T_j = 10°C$ was not included due to intermittent cavitation in the delivery lines causing inconsistent readings.

Upon examining the data for the model case, where

$$T_j = -50°C$$
$$\sigma_j = -5.8$$
$$T_j^* = .26$$

with $\bar{q} = 4$ it can be seen that the profile of the droplet sizes is similar to water with the larger droplets lower in the plume. However, the droplet diameters have been reduced an average of 55% from the water case. The difference in fluid volume would be the fluid comprising the vapor cloud and that which evaporated from individual droplets. By raising the injection temperature to -30°C, σ is increased by 33% and T* is decreased T* by 27%, thereby increasing the rate of evaporation. In doing this, the average droplet diameter at this station drops 10% over the model case. By increasing the injection temperature even further to -10°C, T* is decreased an additional 27% and σ is increased to -0.16 where the Freon is being injected as a nearly saturated liquid.

For this case, the average droplet size is decreased an additional 6% Further examination of the data leads to several observations.

1) By increasing the injection temperature of the Freon-12, it is more readily evaporated, and correspondingly the droplet diameters are reduced.
2) For all cases, the larger droplets occupy the lower section of the plume.
3) As was the case with water injection, increasing the dynamic pressure ratio decreases the mean droplet diameters.

VI. CONCLUSIONS

We return now to the problem addressed in this research, namely understanding how ambient temperature fuel will react in a hot-flow situation before combustion. This information can be provided by the preceding results. The plume can be visualized from the spark shadowgraph pictures of the Freon-12, the atomization and droplet distribution trends throughout the plume can be inferred from the water droplet plots, and an actual idea of the droplet sizes can be gained from the Freon-12 droplet data.

This report shows that the method outlined can be used to simulate a specific case of fuel injection into a heated airstream with chilled fluid injection into an ambient temperature airstream. The process of jet break-up and vaporization can be visualized, and droplet measurements can be made under laboratory environment conditions. This method presents itself as an attractive alternative to complicated and expensive hot flow testing. The introduction of evaporation and heating considerations over a baseline case of water injection can result in a decrease in average droplet sizes by over 70%, while keeping the basic jet structure and break-up mechanisms the same. This demonstrates that evaporation effects are not negligible and should be taken into account when performing injection analyses. Further research in the area should be designed around specific combustor problems in which a quick evaluation of the injection flowfield is needed.

REFERENCES

1. Williams, A., "Combustion of Sprays of Liquid Fuels," The Gresham Press, Old Woking, Surrey, England: 1976.

2. Kush, E. and Schetz, J. A., "Liquid Injection into a Supersonic Flow," AIAA Journal, Vol. 11, No. 9, Sept. 1973.

3. Joshi, P. and Schetz, J., "Effect of Injector Shape on Penetration and Spread of Liquid Jets," AIAA Journal, Vol. 13, No. 9, Sept., 1975, pp. 1137-1138.

4. Baranovsky, S. I. and Schetz, J. A., "Effect of Injection Angle on Liquid Injection in Supersonic Flow," AIAA Journal, Vol. 18, No. 6, 1980, pp. 625-629.

5. Schetz, J. and McVey, W. and Padhye, F., "Studies of Transverse Liquid Fuel Jets in High-Speed Air Streams," V.P.I. - Aero.-0.49.

6. Sherman, A., and Schetz, J., "Break-up of Liquid Sheets and Jets in a Supersonic Gas Stream," AIAA Journal, Vol. 9, No. 4, Apr. 1971, pp. 666-673.

7. Forde, J., Molder, S. and Szpiro, J., "Secondary Liquid Injection into a Supersonic Airstream," Journal of Spacecraft and Rockets, Vol. 3, No. 8, August 1966, pp. 1173-1176.

8. Kolpin, M. A. and Horn, K. P. and Reichenbach, R. E., "Study of a Liquid Injectant into a Supersonic Flow," AIAA Journal, Vol. 6, No. 5, May 1968, pp. 853-858.

9. Schetz, J. A. and Padhye, A., "Penetration and Break-up of Liquids in Subsonic Airstreams," AIAA Journal, Vol. 15, No. 10, October, 1977, pp. 1385-1390.

10. Reichenbach, R. E. and Horn, K. P., "Investigation of Injectant Properties on Jet Penetration in a Supersonic Stream," AIAA Journal, Vol. 9, No. 3, March 1971, pp. 469-472.

11. Nejad, A. S. and Schetz, J. A., "Effects of Physical Properties and Location in the Plume on Mean Droplet Diameter for Transverse Liquid Injection in a Supersonic Air Stream," V.P.I. Technical Paper, 1980.

12. Adelberg, M., "Mean Drop Size Resulting from the Injection of a Liquid Jet into a High-Speed Gas Stream," AIAA Journal, Vol. 6, No. 6, June 1968, pp. 1143-1147.

13. Yule, A. J., "Sprays, Drops, Dusts, Particles", Combustor and Flame, 44:71-84 (1982).

14. Simmons, H. C. and Harding, C. F., "Some Effects of Using Water as a Test Fluid in Fuel Nozzle Spray Analysis," ASME Paper No. 80-GT-90, Dec. 1979.

15. Roberts, J. H. and Webb, M. J., "Measurement of Droplet Size for Wide Range Particle Distribution," AIAA Journal, Vol. 2, No. 3, Mar. 1964, pp. 583-585.

16. Gooderum, P. B. and Bushnell, D. M., "Atomization, Dropsize, and Penetration for Cross Strean Water Injection at High-Altitude Re-entry Conditions with Application to the RAM C-1 and C-III Flights," NASA-TND-6747, July 1972.

17. Dobbins, R. A., Crocco, L. and Glassman, I., "Measurement of Mean Particle Sizes of Sprays from Diffractively Scattered Light," AIAA Journal, Vol. 1, No. 8, Aug. 1963, p. 1882-1886.

18. Mugele, R. A. and Evans, H. D., "Droplet Size Distribution in Sprays," Ind. Eng. Chem., 43, 1951, p. 1317-1324.

TABLE I

Variation of Injection Parameters

T_j(°c)	p_v(psia)	σ_j	T*
-50°	5.7	-5.8	.26
-30°C	14.5	-3.9	.19
-10°C	31.67	-.16	.12
10°C	61.2	6.3	.06

TABLE II

Test Matrix

	Water	FREON-12 T_j = -50°C	F-12 T_j = -30°C	F-12 T_j = -10°C	F-12 T_j = 10°C
$\bar{q}$ = 1					
$\bar{q}$ = 4					

M_∞ = 0.44

P_o = 37 psia

q_∞ = 4.6 psia

To_∞ = 25°C

TABLE III

Droplet Distribution in Plume
Water - $\bar{q}$ = 1 and 4.

Water $\bar{q}$ = 1			Water $\bar{q}$ = 4		
$\bar{x}$	$\bar{y}$	D(μm)	$\bar{x}$	$\bar{y}$	D(μm)
10	3	26.3	10	3	18.7
10	5	18.7	10	6	21
15	3	25.7	10	9	23.3
15	5	19	15	3	20.5
25	3	23.4	15	6	20.2
25	6	17.7	15	9	19.4
50	4	22.3	25	4	24.5
50	8	17.7	25	12	18.7
100	4	22	50	4	23.4
100	8	18	50	8	21.9
			50	8	21.9
			50	12	18.1
			100	4	21.4
			100	8	20.9
			100	12	19.0

TABLE IV

Droplet Profile at $\bar{x}$ = 100
Freon-12, $\bar{q}$ = 4.

	D(μm)		
$\frac{y}{h}$	T_j = -10°C σ_j = -.16 T* = .12	T_j = -30°C σ_j = -3.7 T* = .19	T_j = -50°C σ_j = -5.8 T* = .26
12	<6	6.6	6.7
8	6.7	6.9	7.6
4	8.0	8.4	8.9

TABLE V

Droplet Profile at $\bar{x}$ = 100
Freon-12, $\bar{q}$ = 1.

$\frac{y}{h}$	D(μm)		
	T_j = -10°C. σ_j = -.16 T* = .12	T_j = -30°C. σ_j = -3.7 T* = .19	T_j = -50°C. σ_j = -5.8 T* = .26
5	7.3	8.3	10.4
3	9.1	10.0	10.3

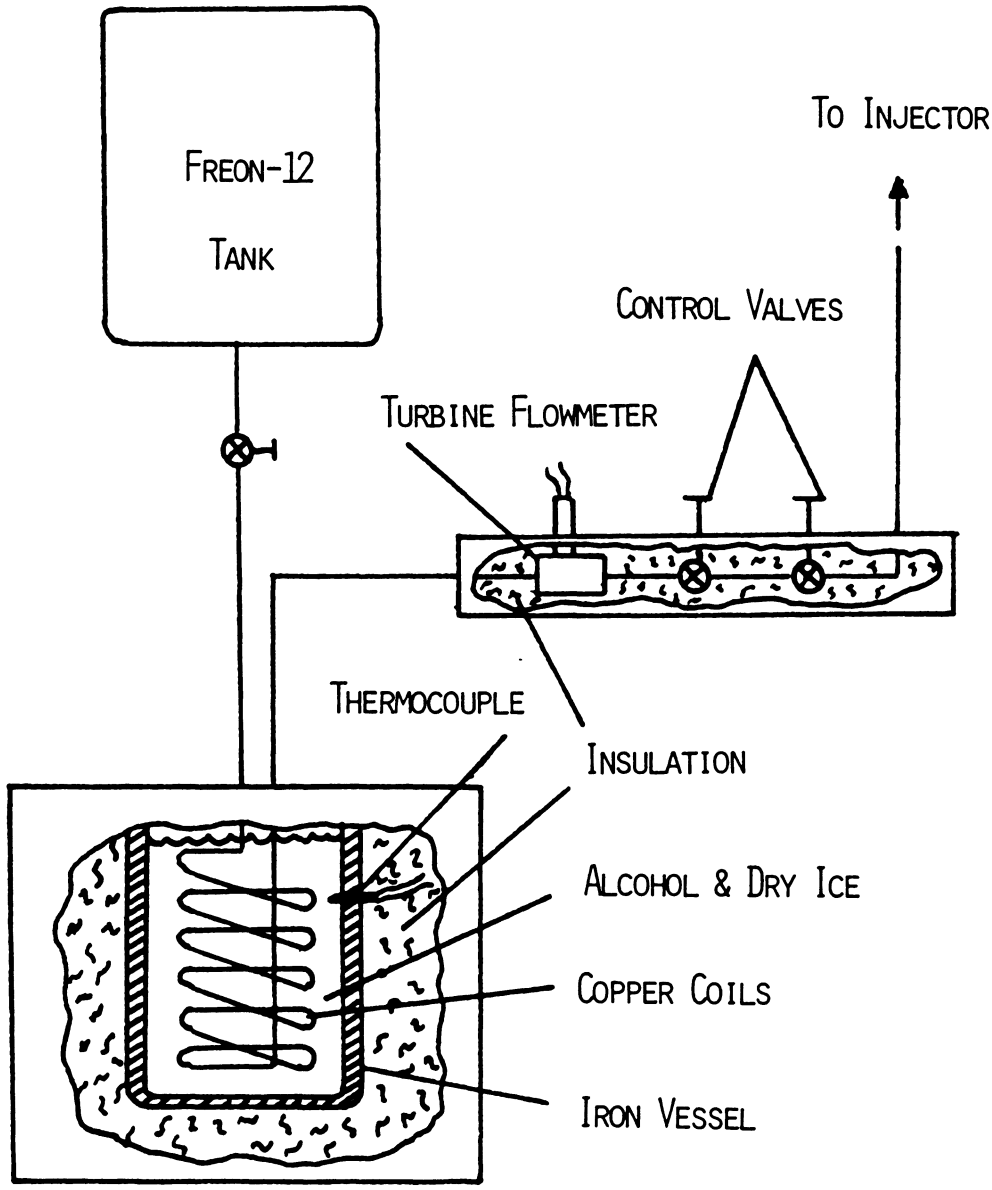

Fig. 1 Freon-12 Delivery System.

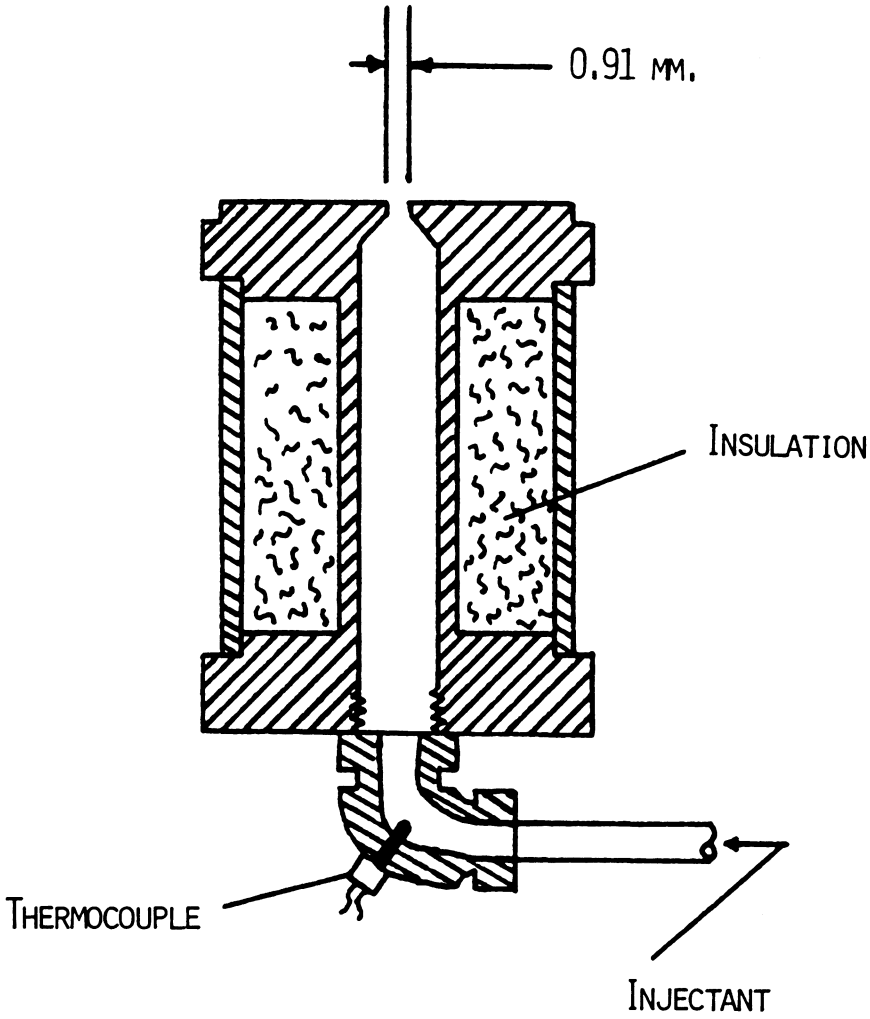

Fig. 2 Injector Assembly.

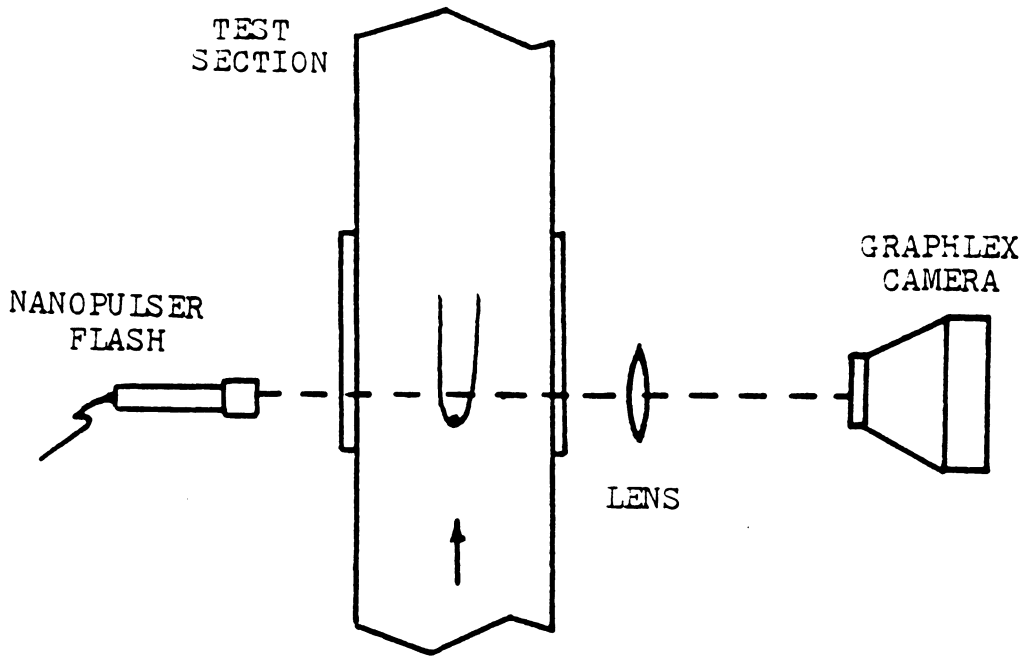

Fig. 3 Spark Shadowgraph Apparatus.

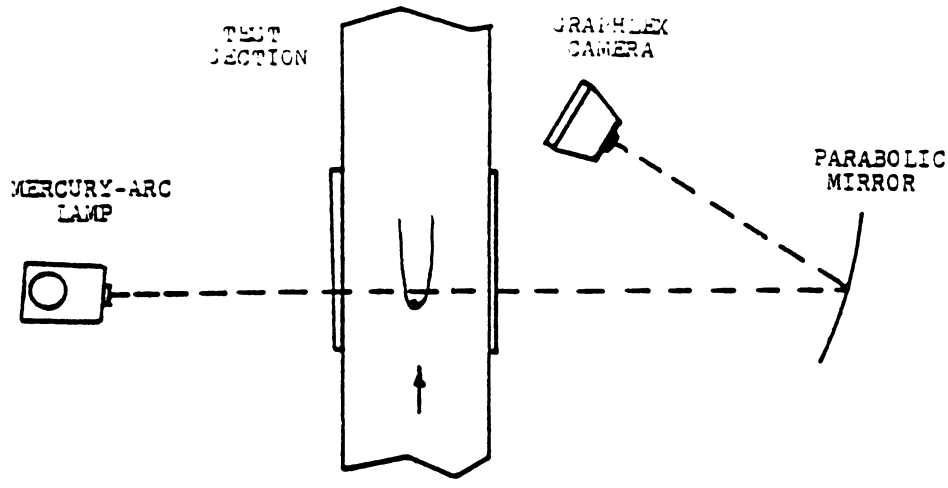

Fig. 4 Streak Photograph Apparatus.

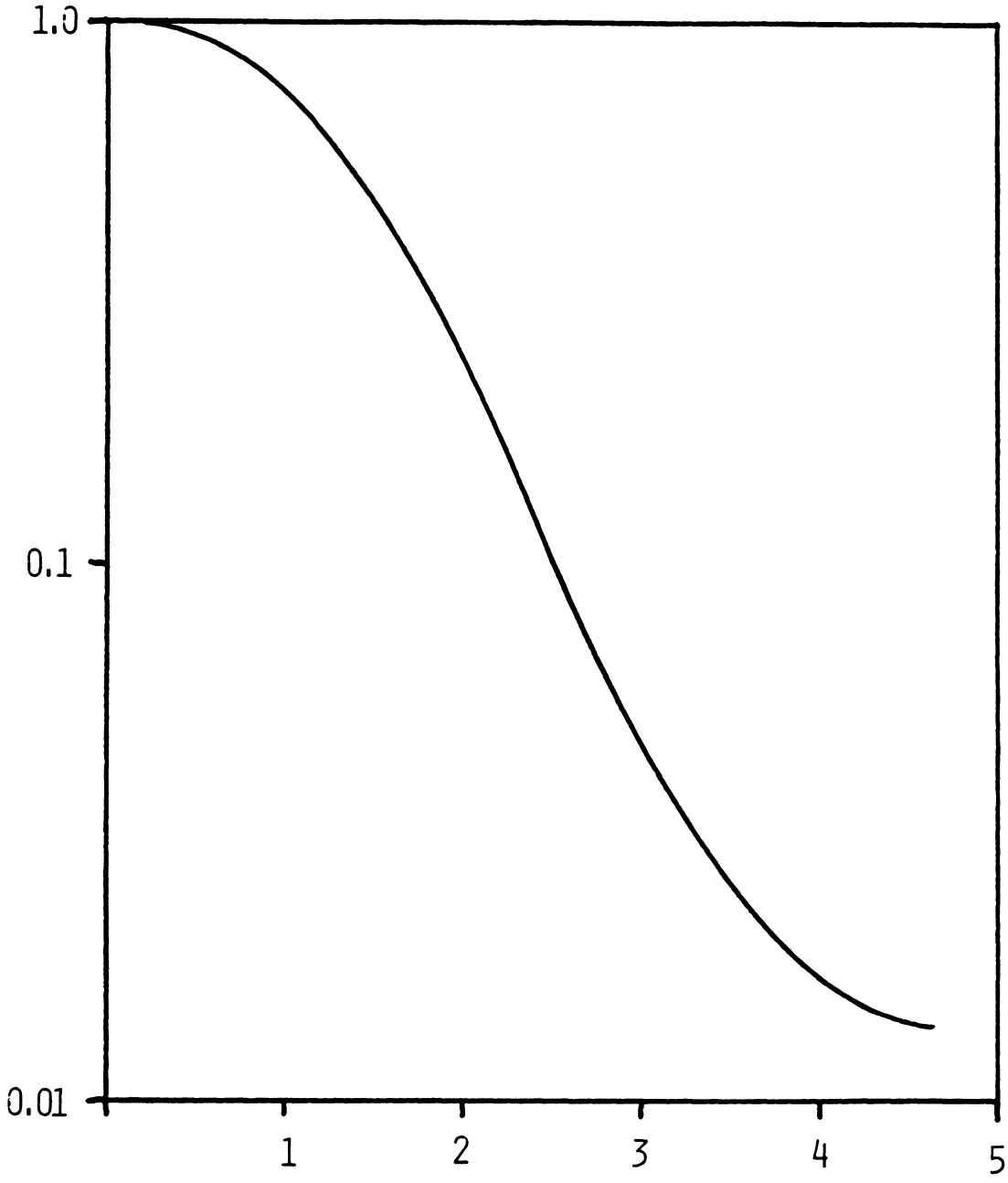

$$\bar{\theta} = \frac{\pi \theta D_{32}}{\lambda}$$

Fig. 5 Theoretical Illumination Profile.

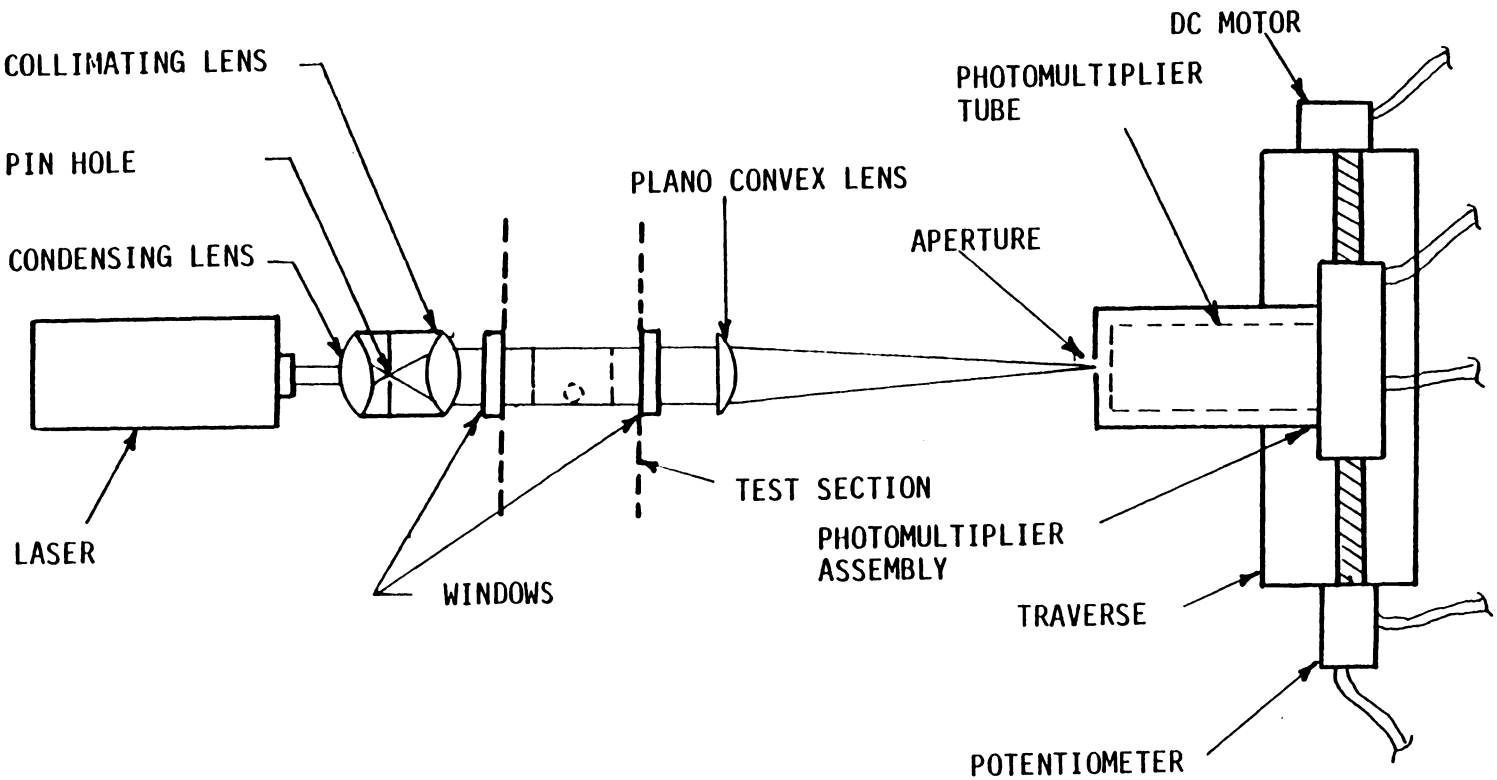

Fig. 6 Optical System for DSLM.

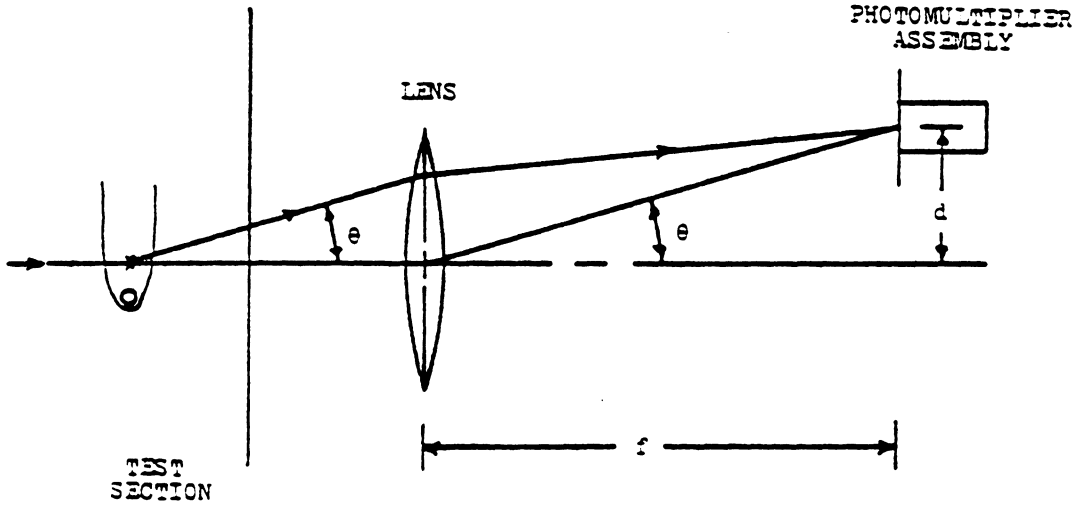

Fig. 7 Optical Arrangement for DSLM.

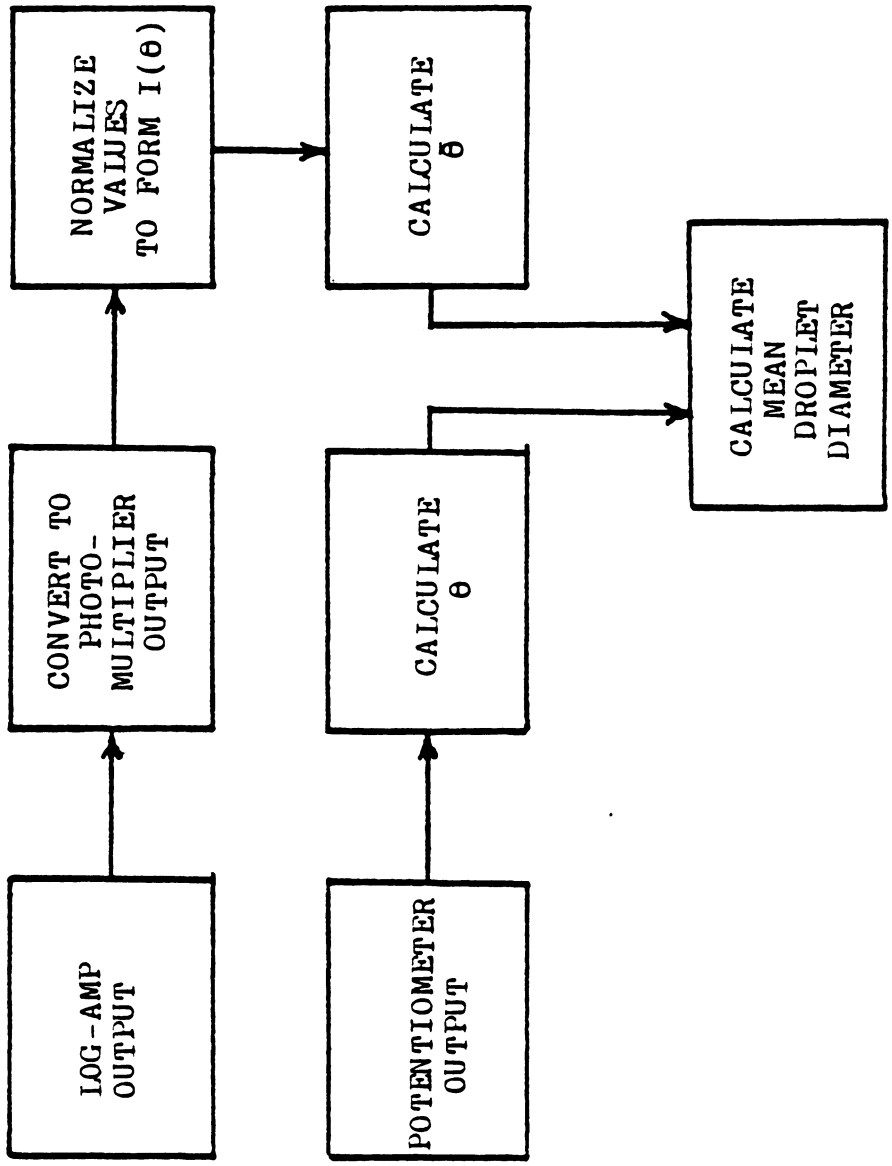

Fig. 8 Block Diagram of Data Processing.

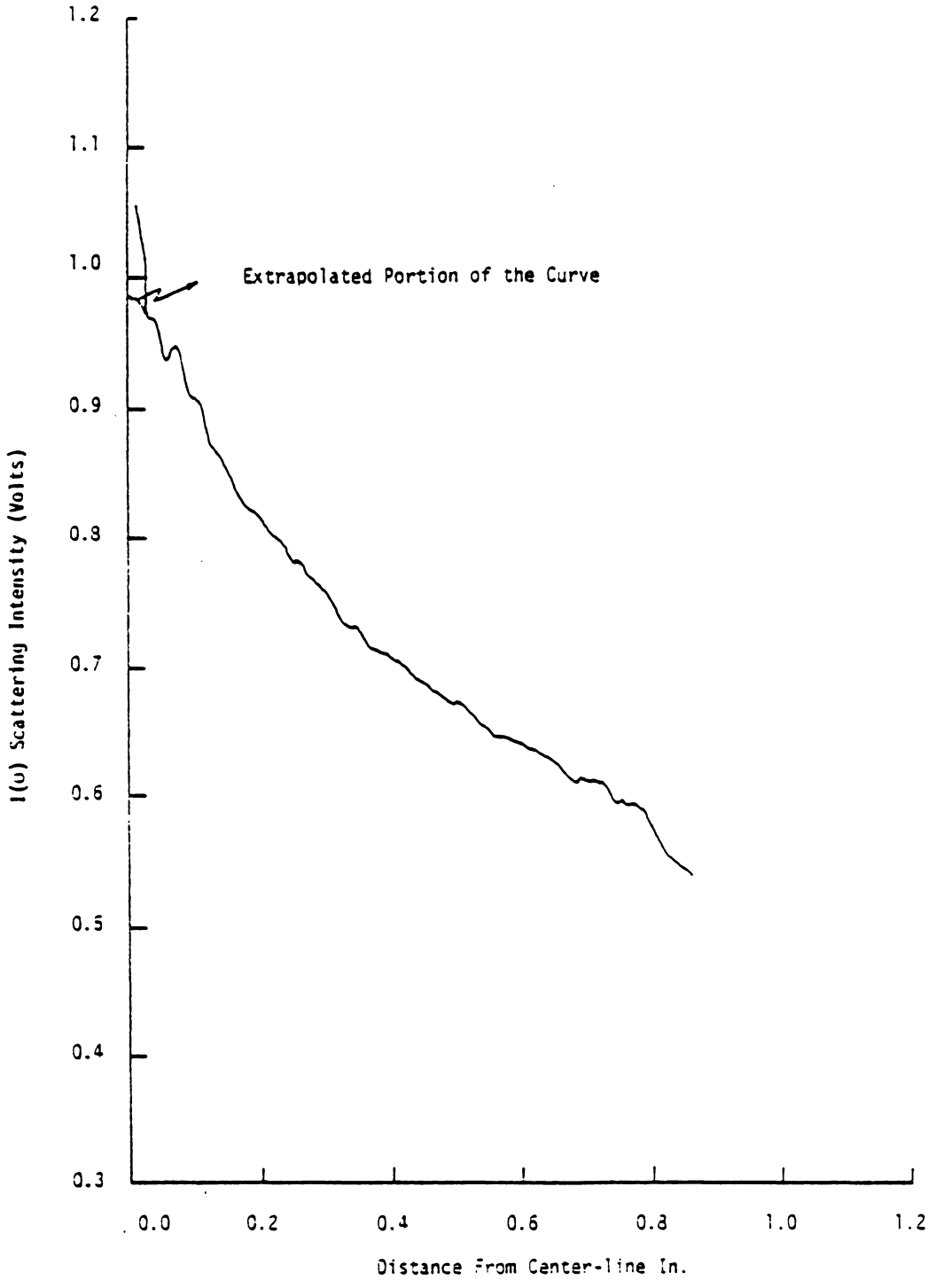

Fig. 9 Versi-Tech Plot of Recorded Data.

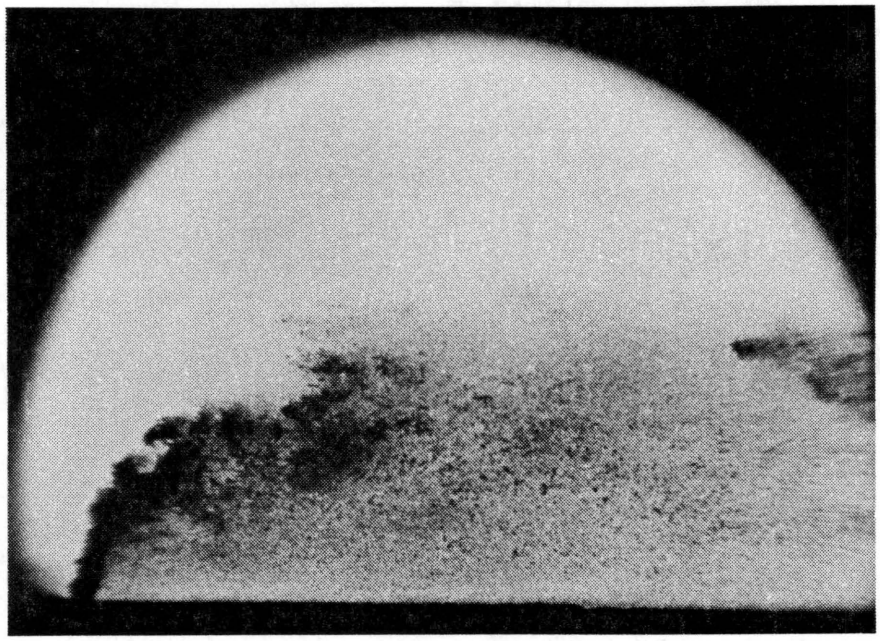

$\overline{q} = 1$

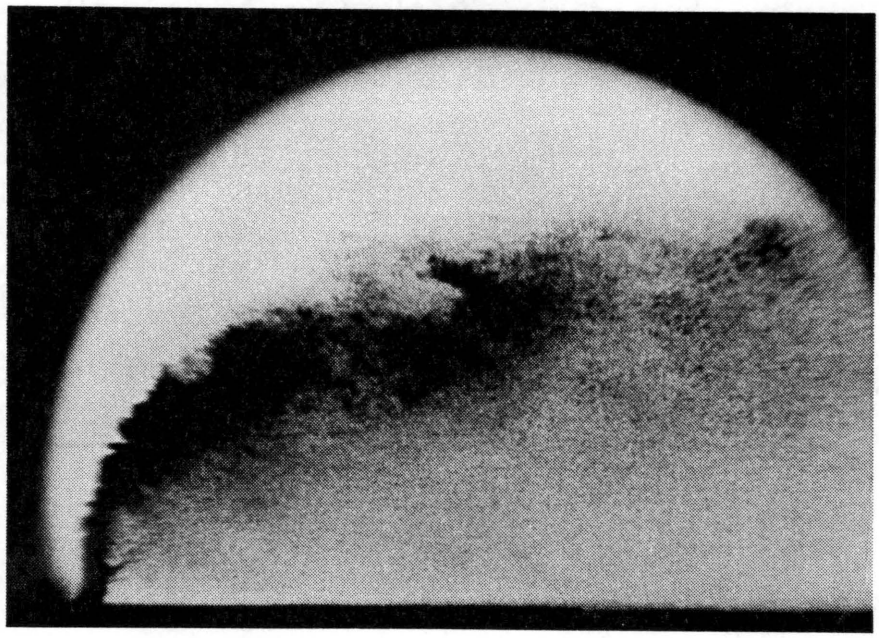

$\overline{q} = 4$

Fig. 10 Spark Shadowgraphs Water - $\overline{q} = 1$ and 4.

(a) T_j = -50°C. σ= -5.8 T*= .26

(b) T_j = -30°C. σ= -3.9 T*= .19

Fig. 11 Spark Shadowgraphs Freon-12 - $\bar{q}$ = 4, T_j = -50, -30°C.

(c) T_j = -10°C. σ= -.16 T*= .12

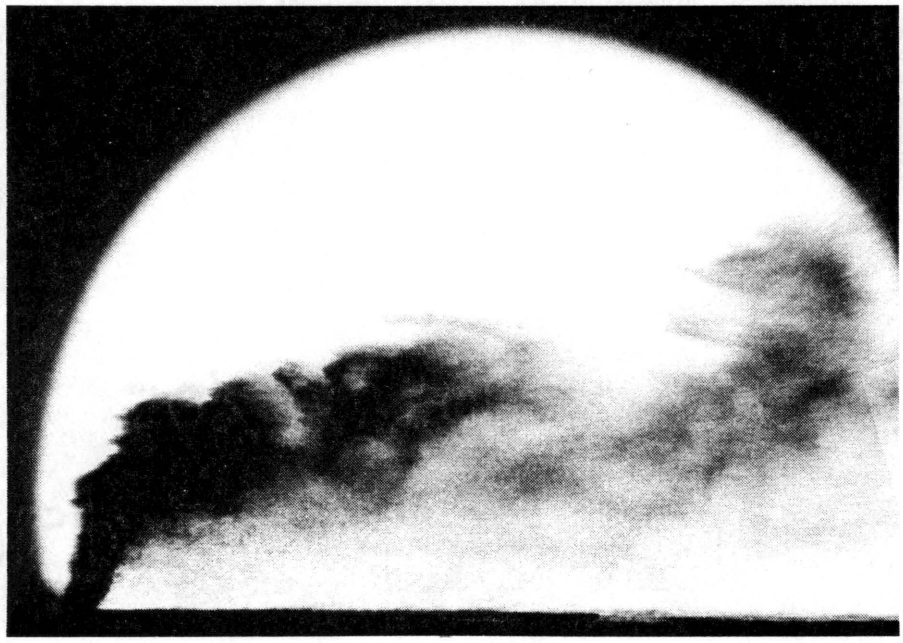

(d) T_j = 10°C. σ= 6.3 T*= .06

Fig. 11, cont'd Spark Shadowgraphs Freon-12 - $\bar{q}$ = 4, T_j = -10, 10°C.

(a) T_j = -50°C. σ= -5.8 T*= .26

(b) T_j = -30°C σ= -3.9 T*= .19

Fig. 12 Spark Shadowgraphs Freon-12 - $\bar{q}$ = 1, T_j = -50, -30°C.

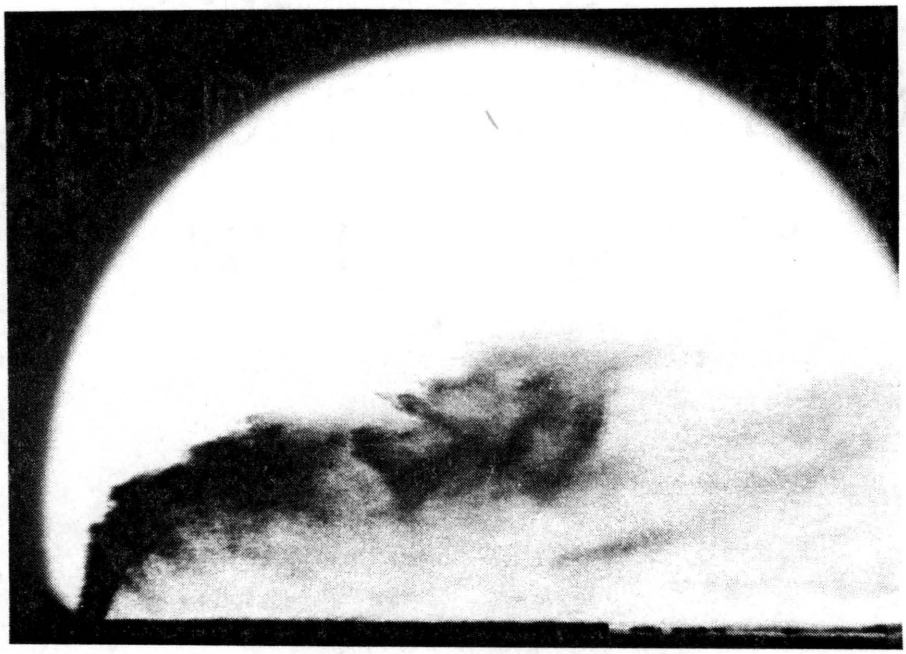

(c) T_j = -10°C. σ= -.16 T*= .12

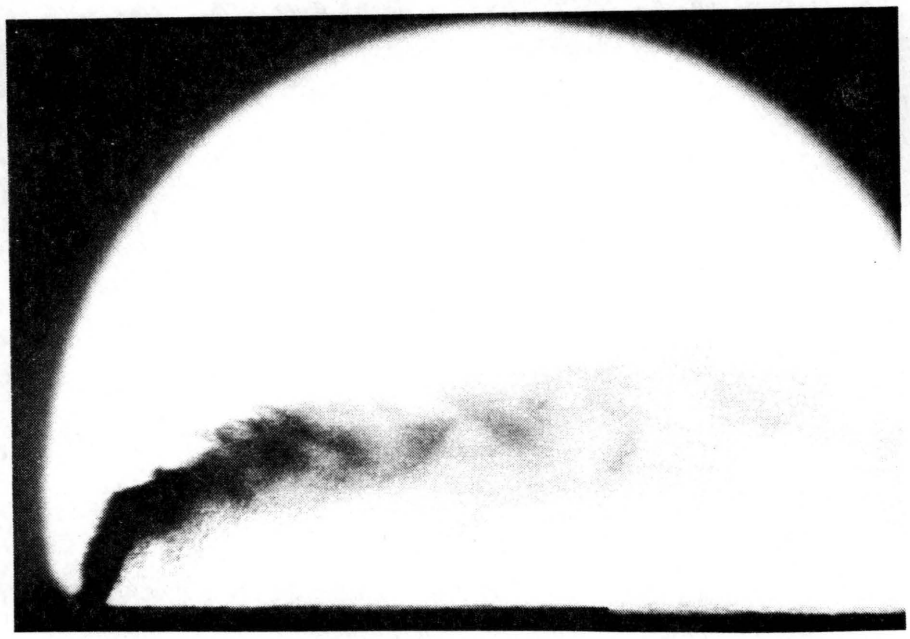

(d) T_j = 10°C. σ= 6.3 T*= .06

Fig. 12, Spark Shadowgraphs Freon-12 - cont'd $\bar{q}$ = 1, T_j = -10, 10°C.

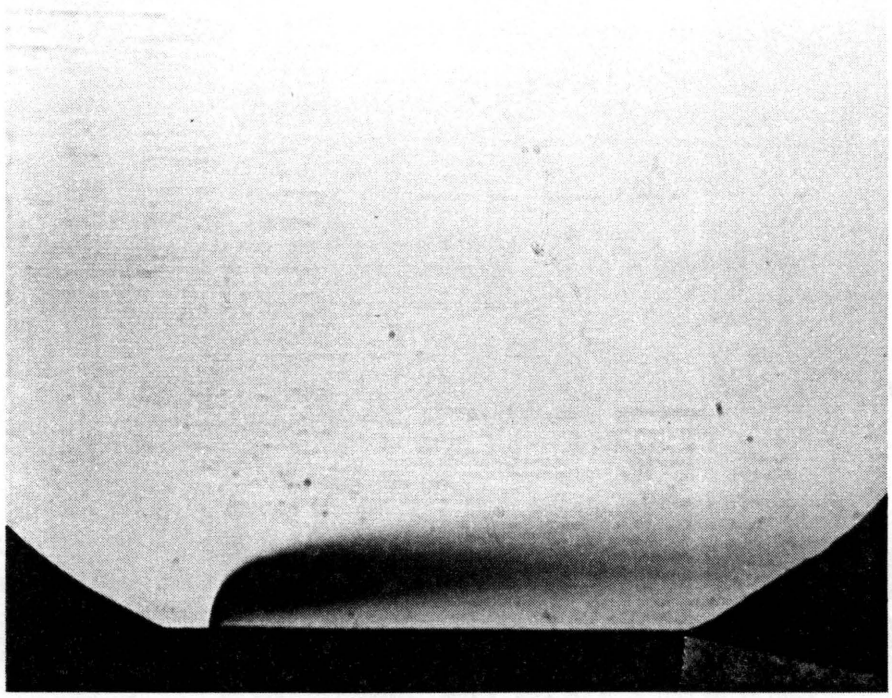

Fig. 13 Sample Streak Photograph.

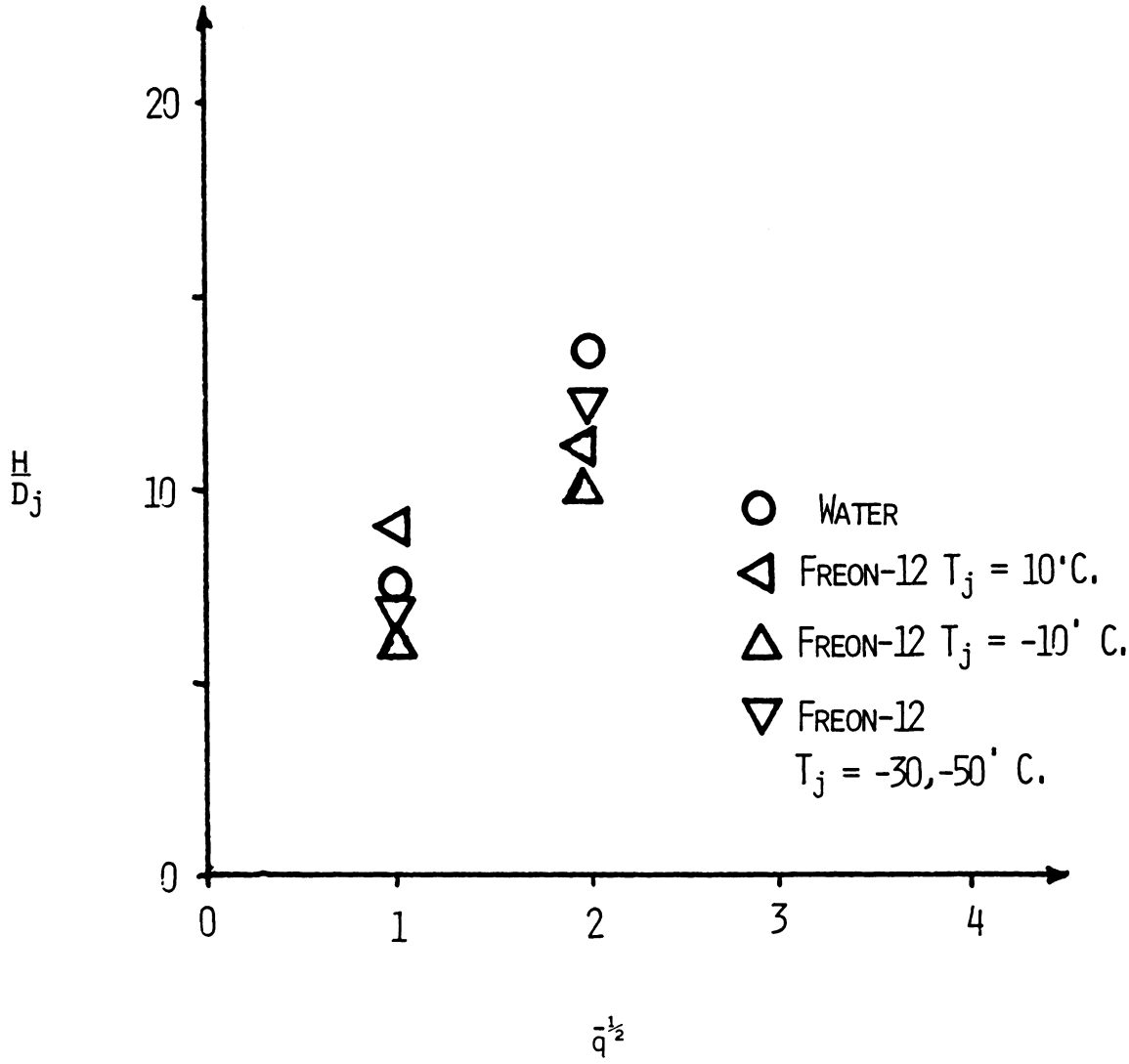

Fig. 14 Penetration Plot of Injectants.

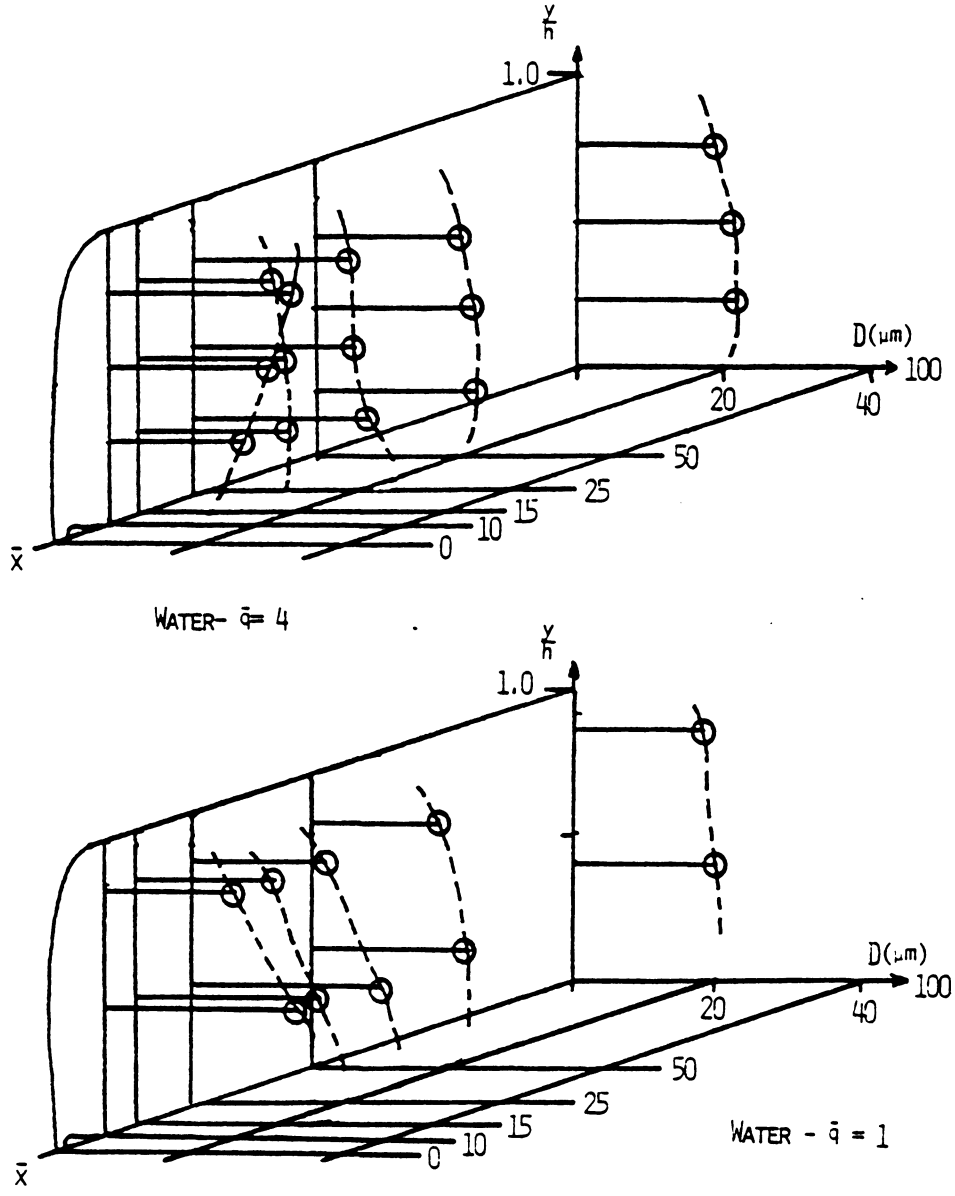

Fig. 15 Droplet Distribution in Plume
Water - $\bar{q}$ = 1 and 4.

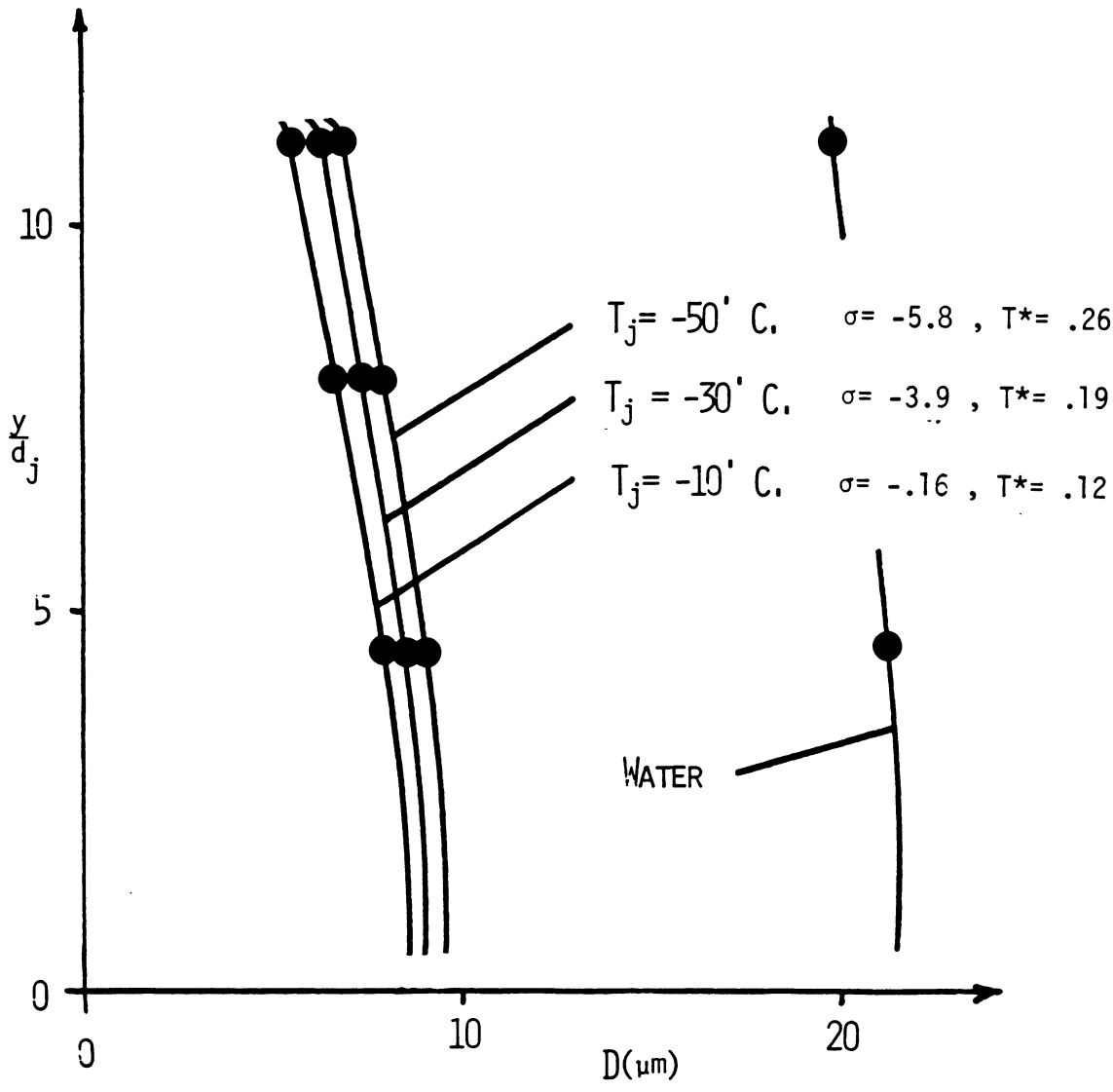

Fig. 16 Droplet Profile at $\bar{x}$ = 100
Freon-12, $\bar{q}$ = 4.

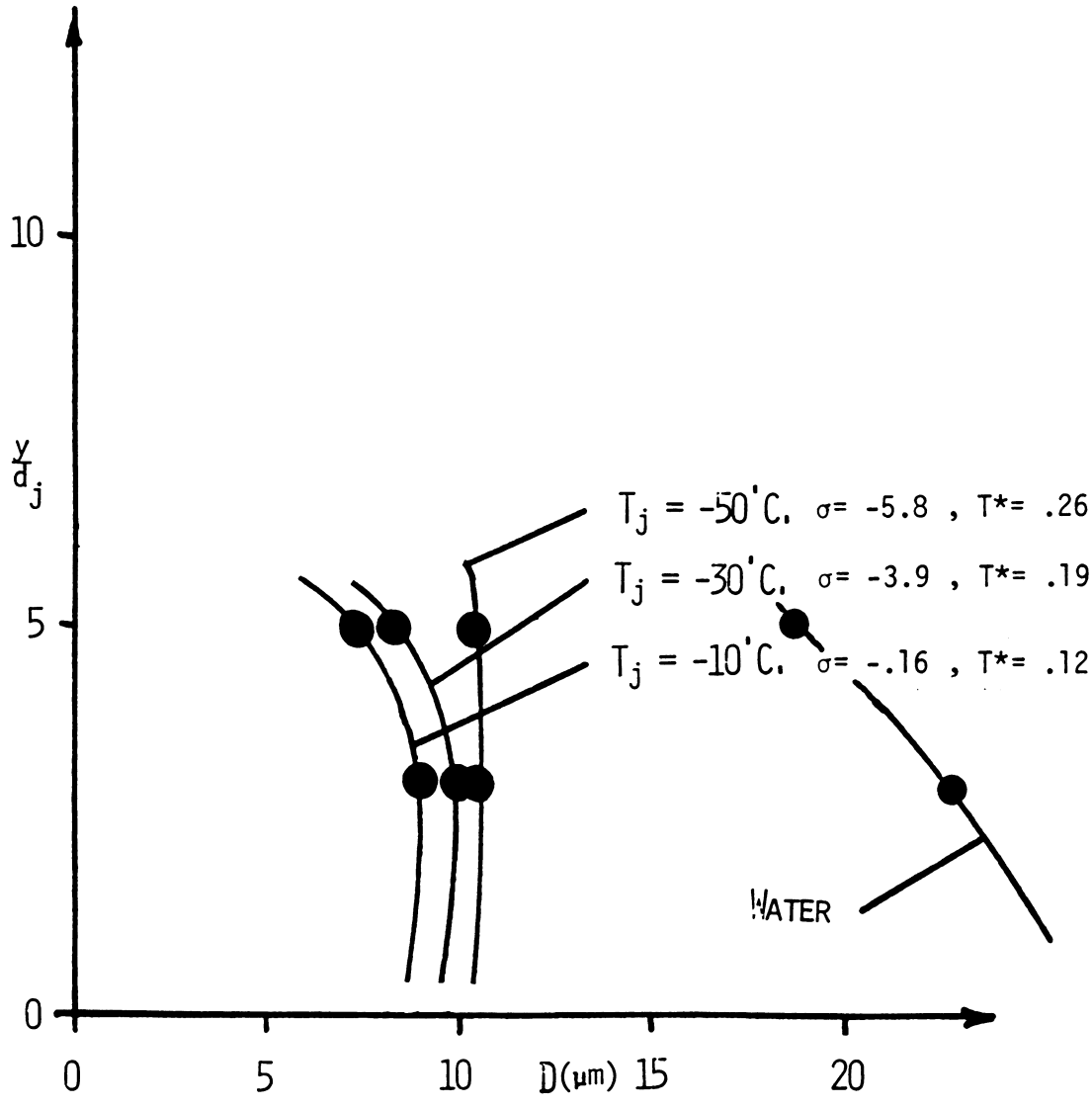

Fig. 17 Droplet Profile at $\bar{x}$ = 100
Freon-12, $\bar{q}$ = 1.

The vita has been removed from the scanned document

AN EXPERIMENTAL SIMULATION OF LIQUID FUEL INJECTION INTO A HEATED SUBSONIC GAS CROSSFLOW

by

Patrick William Hewitt

(ABSTRACT)

In this investigation, an approach to studying hot-flow subsonic cross-stream fuel injection problems with a less complex and less costly cold-flow facility was developed and implemented. An actual ramjet combustion chamber fuel injection problem was proposed where ambient temperature fuel was injected into a heated airstream. This case was transformed through similarity parameters involving injection and freestream properties to a simulated case where a chilled injectant was injected into an ambient subsonic airstream. This task was accomplished through injection of chilled Freon-12 into the Virginia Tech 23 x 23 cm. blow-down wind tunnel at a freestream Mach number of 0.44. The freestream stagnation pressure and temperature were held at 2.5 atm. and 300^{o}K respectively. The resulting spray plume was carefully examined and documented with photographs and droplet measurements. The results showed a clear picture of the mechanisms of jet decomposition and vaporization. Immediately after injection a vapor cloud was formed in the jet plume, which dissipated downstream leaving droplets on the order of 8 to 10 microns in diameter for the conditions examined.